

Identification of Power BJT Operating Stages Based on Experimental Excess Charge Estimation*

1st Given Name Surname
dept. name of organization (of Aff.)
name of organization (of Aff.)
City, Country
email address or ORCID

2nd Given Name Surname
dept. name of organization (of Aff.)
name of organization (of Aff.)
City, Country
email address or ORCID

Abstract—The paper proposes and demonstrates an experimental way of estimating the amount of stored charge of excess minority carriers within power BJT base and collector. This consequently allows a detailed identification of transistor operating stage.

A brief device operation analysis is provided as a clear support of the measured characteristics.

The method is based on determining the steady-state stored charge at various operating conditions by integration of negative transient base current during turn-off event which deflates the stored charge.

An ultimate objective of these and future experiments is an accurate interpretation and modelling of various device stages during IGBT switching process. Most of the observed phenomena are common among a power BJT and IGBT's intrinsic BJT. As IGBT doesn't provide access to the internal base current, it is advantageous to interpret the relations between stored charge and switching waveforms of power BJT first and further generalize the observations to latter IGBT measurements.

Index Terms—IGBT, power BJT, bipolar semiconductor devices saturation, minority carriers concentration, excess charge storage, transistor switching measurement,

I. INTRODUCTION

Devices utilizing bipolar current transport used as a fast power switches such as IGBTs are not going to be fully replaced by unipolar counterparts in the near future thanks to their high current density capability at optimum manufacturing price. Notorious downside of bipolar devices is charge storage within forward-biased junctions, limiting the switching speed.

High current density is allowed by two phenomena unique for bipolar devices physics (i.e. including the minority carriers action) - the saturation and conductivity modulation in lightly doped region. Both are related to minority carriers charge storage and dependent on the base and collector current levels. As a result, the good on-state performance can be achieved at the cost of degrading the switching performance and vice-versa. In addition, the charge storage undesired side-effects are clearly reflected in the switching waveforms [1].

Saturation mode is essential for steady on-state operation as described by a static current - voltage characteristic. It is defined by excess minority carriers concentration within the base and collector during forward bias of both BJT

junctions. While there is only a little practical significance in determining the amount of excess charge stored in the collector for static saturation characteristic analysis of already-manufactured device, estimating the boundaries of individual operational modes is highly beneficial for accurate identification and analysis of particular stages during switching action. However, determining the amount and geometric profile of excess charge stored in the collector N-drift region is not trivially possible by means of static saturation characteristic measurement. On the other hand, the excess charge - continuously recombined with majority carriers - is supplied by the base current. Likewise, negative base current can be utilized to deflate the excess charge. So, one only need the access to the base current transient switching waveform and to eliminate the recombination impact on measured waveform to gain a quantitative information about the steady-state minority carriers stored within transistor right before the switch-off event. Unfortunately IGBT doesn't provide access to the internal base current, but most of the phenomena in question are common among a power BJT and intrinsic BJT within IGBT. It is thus beneficial to use an "archaic" power BJT as a qualitative testing reference with the advantage of direct control of base current parameters, waveform shape and its accurate measurement.

The gained observations can be further almost-directly applied to the IGBT on-state and switching waveforms interpretation [2].

Measurements presented in next sections were performed to experimentally validate the possibility to interpret the power BJT operational stages by estimating the amount of base and collector stored charge of excess minority carriers based on base current transient waveform measurements. In other words, to validate the following presumptions:

- Recombination of minority carriers is at least one order of magnitude slower than times required for external deflation of the excess charge (i.e. the turn-off time),
- Basic function of power BJT is given primarily by the desired "theoretical" phenomena prior to the undesired side-effects.

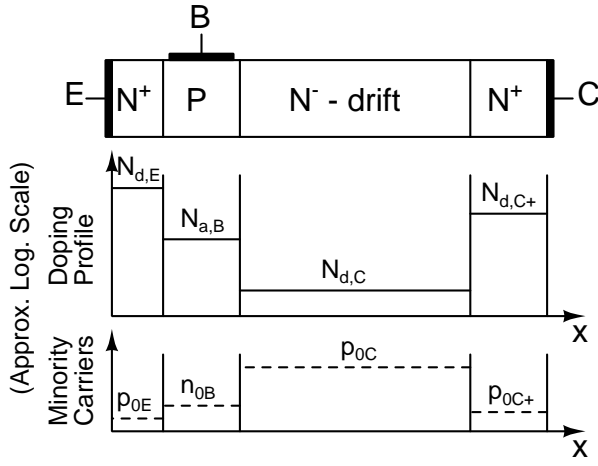


Fig. 1. Structure of power BJT. Dimensions and concentrations scale are illustrative i.e. not proportional to real scales.

II. A BRIEF THEORY

A. Structure of Power BJT

The basic one-dimensional structure of power BJT is depicted on Fig. 1. It approximates the cross-section of a real device right beneath the emitter contact. Unlike a low voltage BJT, the structure involves a very lightly doped so-called drift region in the collector to support high collector voltage by the depletion region while reverse biased. The current flow through drift region creates additional voltage drop unless being flooded with injected minority carriers exceeding the equilibrium concentration multiple times (conductivity modulation [2]). The minority carriers concentration in equilibrium within doped semiconductor with intrinsic carrier concentration n_i and doping concentration N_D or N_A is given by:

$$n_{p0} = \frac{n_i^2}{N_D}, \quad p_{n0} = \frac{n_i^2}{N_A} \quad (1)$$

The higher doping, the lower minority carriers concentration as depicted on Fig. 1.

B. Operation of power BJT

Bipolar transistor operates in 3 basic modes, corresponding to 3 combinations of biasing 2 junctions within the transistor, as summarized in Tab. I. This can be considered as opera-

Mode	B-E bias	B-C bias
Cutoff	R	R
Active	F	R
Saturation	F	F

TABLE I
Caption text

tion mode definitions. Corresponding illustrative (not properly scaled) minority carrier concentrations and potentials within device structure are depicted on Fig. 2. The minority carrier concentrations on the junction (depletion region) boundaries - let us denote it $p_n(0)$ and $n_p(0)$ - adhere the following principles:

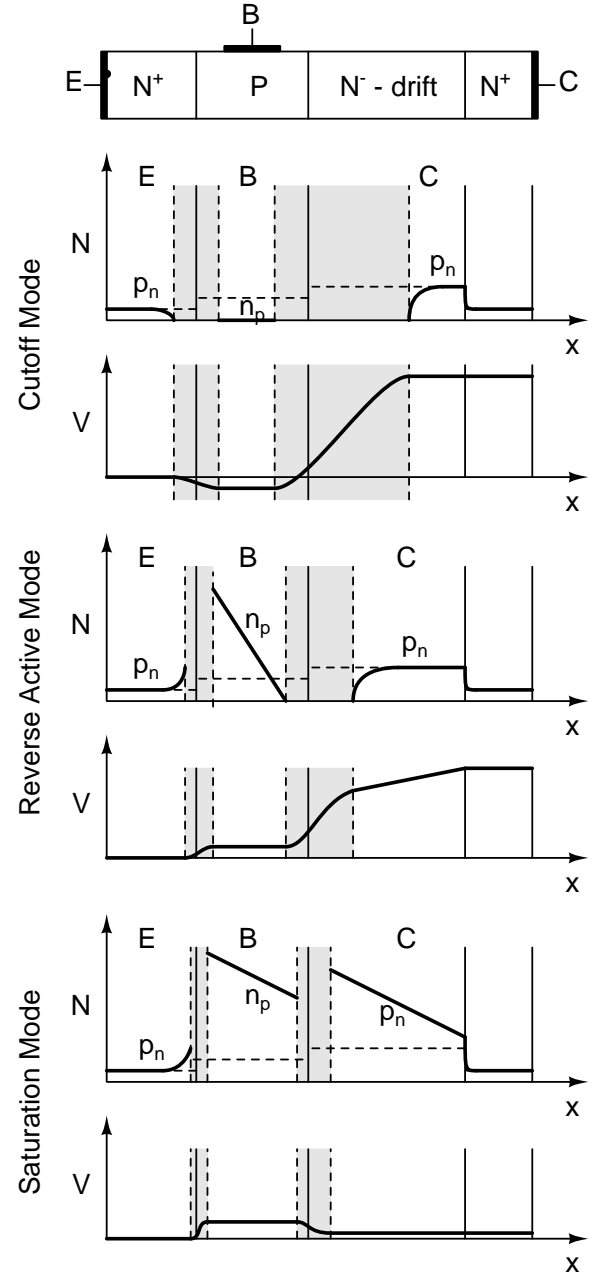


Fig. 2. i++i

- reverse biased junction:

$$p_n(0) = 0, \quad n_p(0) = 0 \quad (2)$$

- forward biased junction: "The Law of Junction" [3]:

$$p_p(0)n_p(0) = n_i^2 e^{qV_{PN}/kT} \quad (3)$$

$$n_p(0) = n_{p0} \cdot e^{qV_{PN}/kT} \quad (4)$$

$$p_n(0) = p_{n0} \cdot e^{qV_{PN}/kT} \quad (5)$$

Shaded area represents the depletion region.

Carriers concentration gradient signifies the diffusion current while the potential (voltage) gradient signifies the drift

current. Drift current (and thus the voltage gradient - i.e. also the capability to support voltage) is typical for depletion regions and lightly doped region without conductivity modulation. In fact, the drift current principally signifies the current flow through the resistance in general.

In active mode, the B-E junction is forward biased, which results in minority carriers injection from emitter into the base region (the “Law of junction”) and B-C junction is reverse biased resulting in zero electron concentration at the junction. The current flows through the collector despite the reverse bias, due to minority carriers diffusion at the depletion region margin (carriers gradient within base) and drift through the depletion region (potential gradient within depletion region). The minority carriers in collector does not exceed the equilibrium concentration.

Collector voltage (with respect to the emitter) can be varied by varying the depletion width. In other words, varying the resistivity of the current path.

In saturation mode, both junctions are forward biased. N-drift region is flooded with minority carriers injected from the base, exceeding an equilibrium concentration, typically exceeding even the majority carriers equilibrium concentration. Consequently the majority carriers concentration is increased as well to maintain charge neutrality [2]. As a result, low doping causing additional voltage drop while proportional to the collector current is effectively increased and voltage drop disappears. This is called the *conductivity modulation*.

Thus, there is no significant drift current, the collector current is maintained by diffusion. As stated before, drift signifies the resistive material, while transistor in saturation exhibits the low-resistivity (on-state) performance. Carrier concentration gradient is equal for base and collector region as depicted on Fig. 2 guaranteed by the same (diffusion) current I_C .

C. Active and Saturation Mode at Various Conditions

Poriadne ale stručne tu popísať este Fig. 3 - hlavne izrejme závislosti naboja (gradient aj celkové množstvo) na I_C a I_B . Z toho potom vychádzajú merania. – skaly su rozdielne na obr. bazy a kolektora. V aktivnom režime sa uskladňuje a vyprazdňuje oveľa menšie množstvo naboja (horný obr.), ako v saturacnom (spodný obr), preto su zmeny v aktivnom režime ďaleko rýchlejšie, ako v pomalom saturacnom. - tiež beta (akt., sat.) - vrátane charge control rovnice.

D. Charge Control Relation

Qualitative considerations in section II-C regarding the stored charge within base and collector can be supported by simple yet accurate enough *charge control* relations [4], [5] as follows:

$$\frac{dQ}{dt} = i_B(t) - \frac{Q(t)}{\tau} \quad (6)$$

where Q denotes the total stored charge, i_B is the base current supplying (or deflating) the charge and τ stands for the recombination time constant - i.e. Q/τ represents the “recombination current”, proportional to amount of stored charge [3].

All excess minority carriers charge is supplied by the base current and it is not necessary to partition i_B into individual parts (i_{pC} etc.) as it is not needed to identify individual portions of total stored charge.

In steady state, I_B is just sufficient to supply the recombined charge (proportional to total stored charge volume):

$$I_B = \frac{Q}{\tau} \quad (7)$$

which describes all 3 modes in Tab. I. $I_B = 0$ in cutoff mode so stored charge equals zero; $I_B > 0$ which signifies the forward bias of B-E junction in active and saturation mode further defined by collector bias voltage.

Negative base current is not possible in steady state.

aj z tohto vidno, že zmeny v aktivnom režime prebiehajú omnoho rýchlejšie, ako v saturácii.

potom sa bude asi uvažovať že Q_C je hlavná časť celkového Q odsateho bazovým prúdom, a ostatné časti sa oproti nej zanedbávajú.

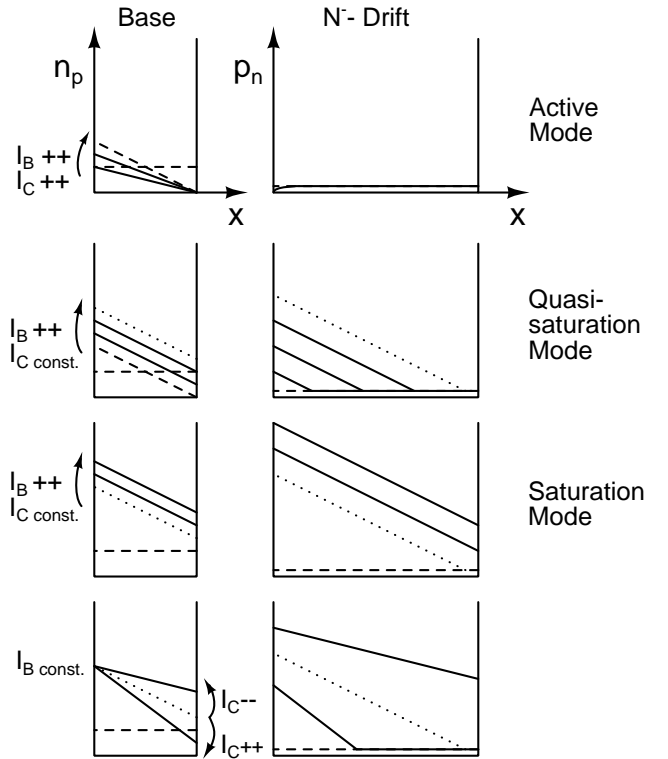


Fig. 3.

III. METHODOLOGY

A. Negative Base Drive Transient Current Relation with Stored Charge

As stated before, negative base current is not possible in steady state. However, it is extremely useful to apply a negative transient base current during turn-off event to speed up the charge deflation from base and collector.

vysvetlit znamienka a celkovo to integrovanie co znamena pre meranie

- vplyv rekombinacie
- nerovnost skutocneho ustaleneho Q_{ss} a meraneho Q_{ssm}

Integration of the “discharging” analogy to (6) yields:

$$Q_{ss,m} = \int i_{B-}(t) dt = Q_{ss} - \frac{1}{\tau} \int Q(t) dt \quad (8)$$

That is, the obtained steady-state charge projection $Q_{ss,m}$ (“m” stands for “measured”) is not necessarily equal to an actual stored charge Q_{ss} . The difference between those two is the portion of charge that already got recombined.

$$Q_{ss,m} = Q_{ssa,actual} - Q_{recomb}. \quad (9)$$

B. Test Summary

There are two quantities, the actual steady-state Q_{ss} stored in the collector and its measured projection $Q_{ss,m}$ (“m” stands for “measured”). They are both dependent on varying test conditions like I_{B+} , I_{B-} , I_C , either directly (Q_{ss} , according to (7) and Fig. 3) or indirectly ($Q_{ss,m}$) through the deflation time (t_{defl}).

The following experimental tests were proposed based on above analysis. To be noted, all of the tests are based on steady-state stored charge quantification at varying conditions.

- Q vs. I_{B+} at constant I_{B-} , I_C
 ucel
 ockavanie - linearny narast podla rovnice XYZ
- Q vs. I_{B-} at constant I_{B+} , I_C
 ucel - overit pri jakom I_{B-} sa da povazovat $Q_{ss}=Q_{ss,m}$
 ockavanie - konstantna char., s rastucim casom (klesajuci I_{B-}) klesajuca k nule
- Q vs. I_C at constant I_{B+} , I_{B-}
 ucel
 ockavanie - lin. pokles az po akt. oblast

C. Test Bench

odkaz na diplomovku a prochazku, switching measurement, minimized parasitic influence

DUT

budenie cez R_{b+} , R_{b-} , konst. I_b

zataz

All testing was performed on test bench built for fast switching measurement of power semiconductor devices with minimized parasitic influences as described in [6] and [7] in detail.

The device under test - power BJT BUV48A - was driven by discrete base driver through a variable base resistor to provide a constant I_{B+} during whole “charging” on-state period and constant I_{B-} during most of the “discharging” turn-off event. Separated current path and base resistors were ensured for I_{B+} and I_{B-} via diodes.

IV. MEASUREMENT AND INTERPRETATION OF RESULTS

rozdelenie Q na Q_1+Q_2 - vid aj textak pozn K popiskom obrazkov nezabudnut pripojit podmienky (i_{b+} , i_{b-} , i_c)!!!

A. Q vs. I_{B+}

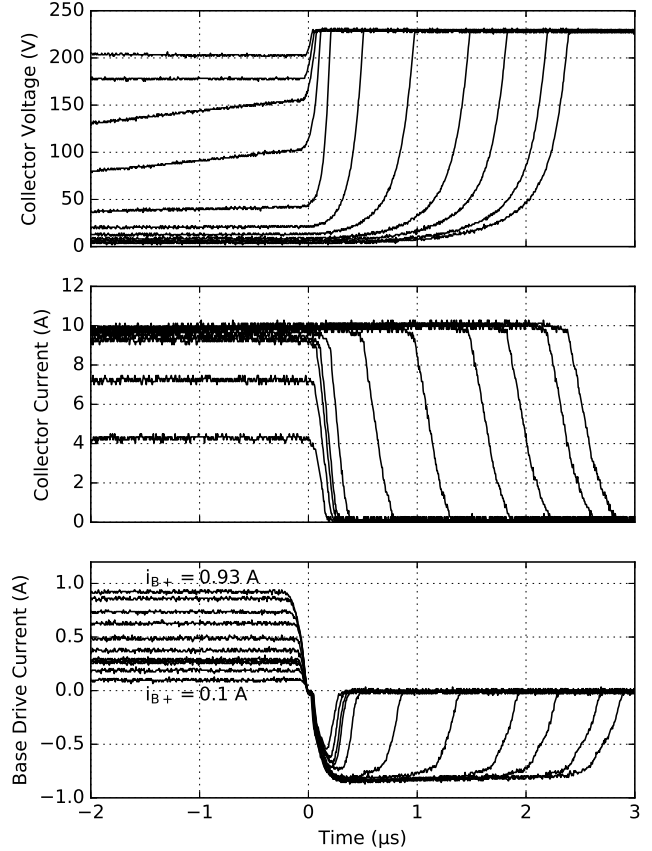


Fig. 4. i_{b+}

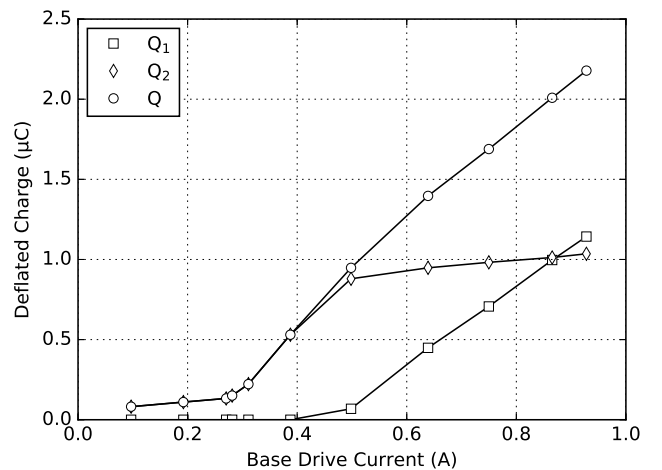


Fig. 5. i_{b+}

- podľa očakávania a rovnice (xyz) je to linearna charakteristika pokiaľ je v saturacnom rezime
 - linearna je aj v aktivnom, pricom v aktivnom sa uskladnuje omnoho menej naboja - iba v baze - hranicu medzi aktivnym a saturacnym rezimom dokaz o aktivnom rezime okrem jasneho zlomu v priebehu $Q=f(I_{B+})$ je aj pohľad na priebehy i_B a i_C . vidno ze i_C dokonca je mensie nez meracie podmienky. to kvoli tomu, ze s takym malym i_B mu beta nedovoli byt vacsi - namiesto toho stupne napatie. Beta sa da aj lahko vycilit - $i_C/i_B = 4/0.1 = 40$. ??? (vyrobca udava min. 8), ale pri podmienkach zodpovedajucich saturacii - takze neviem naco vobec udava betu

- vycislit aj naboje v aktivnom rezime
 - vysvetlit, preco Q_2 je od urcitej hranice konstantny

B. Q vs I_{B-}

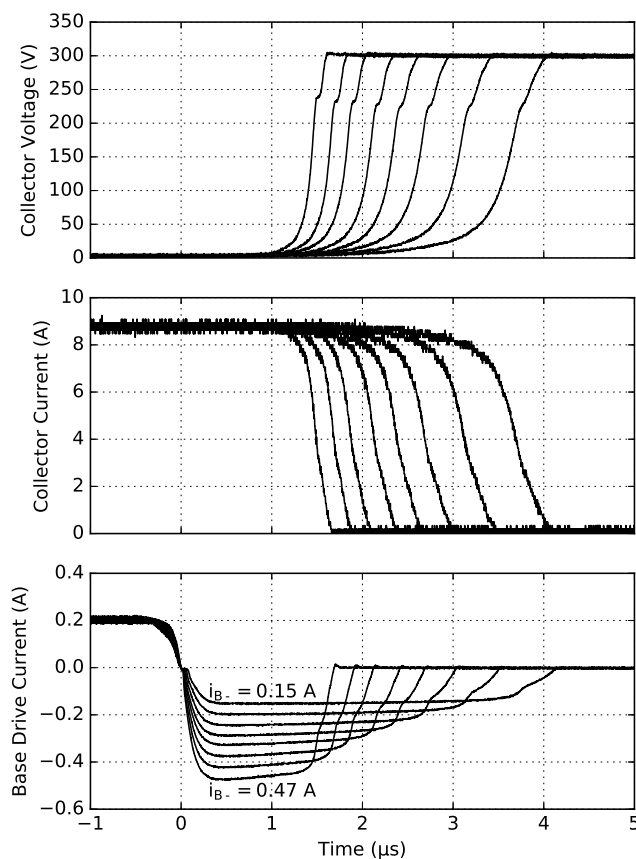


Fig. 6. i_{B+}

podľa očakávania su pre dostatočne veľké I_{B-} krivky konstante (nezavisle na I_{B-}).

tiez podľa očakávania so zmeňujúcim I_{B-} (tj. vzrastajúci čas odsávania, a tým aj rekombinácie) zmerany naboje klesá smerom k nule.

Dôležité pozorovanie je aj to, že Q_2 je "konstantnejší" než Q_1 . Z toho je zreteľne vidno že:

- rekombinácia prebieha hneď od začiatku (čo je aj samozrejme). Žiadne take, že až keď začína klesať prúd (i_B , i_C),

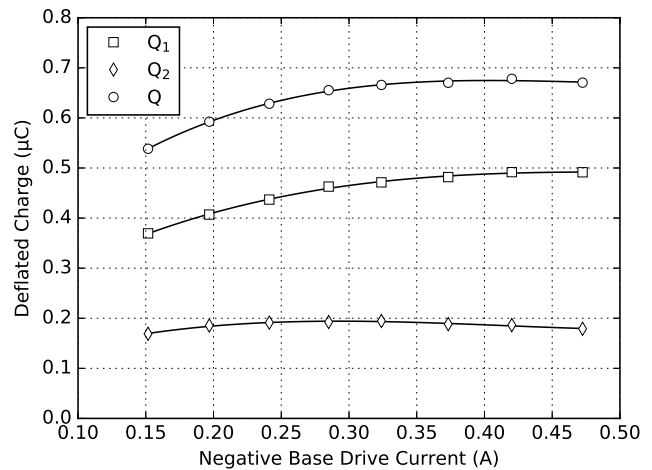


Fig. 7. i_{B+}

vzrastat napätie na prechode alebo take niečo.

- rekombinácia je umierna celkovému naboju, tak ako ukazuje rovnica (6). Po odčerpaní Q_1 je už celkového naboja menej, ale odsávaný prúd zostáva rovnako veľký. β pomer rekomb. ku odsávaniu sa zmenšil, preto krivka zmeraného naboja klesá pomalšie (menej ju kazí rekombinácia)

C. Q vs I_C

-podľa očakávania z obr. 3 sa s rastúcim I_C uložený naboje ZMENSUJE

-dokonca pekne lineárne, čiže v tomto meraní sa podarilo podľa plánu eliminovať nepresnosť merania spôsobenú rekombináciou. A zároveň to potvrdilo, že hlavné javy v tranzistore sú tie, ktoré sú žiadané a viditeľné aj zo zjednodušených predstáv a modelov, nie nejake vedľajšie a parazitné.

-Ďalej tiež celkom pekne vidno hranicu aktívneho a (kvazi)saturacného režimu. A naboje v aktivnom režime - zodpovedajúci naboje iba v baze - veľkosťou súhlasí s tým, čo vyšlo z merania Q vs. I_{B+}

V. CONCLUSION AND FUTURE WORK

stručne zhrnutie, že meranie naplno potvrdilo predpokladané závislosti z teoretickej analýzy.

do budúcnosti:

Q vs I_C pre viacere I_B

porovnať buďenie cez R, L, (C), s antisat. diódou (aj keď neviem či zrovna machrovať s tým, že to ešte nie je úplnosť)

REFERENCES

- [1] C. Hu and M. J. Model, "A model of power transistor turn-off dynamics," 1980 IEEE Power Electronics Specialists Conference, Atlanta, Georgia, USA, 1980, pp. 91-96.
- [2] B. J. Baliga, Fundamentals of Power Semiconductor Devices, New York: Springer, 2008.
- [3] R. F. Pierret, Semiconductor Device Fundamentals, Addison-Wesley Publishing Company, 1996, ISBN 0-201-54393-1
- [4] Gummel
- [5] S. M. Sze and M. K. Lee, Semiconductor Devices: Physics and Technology, 3rd ed., New York: John Wiley & Sons, Inc. 2012.

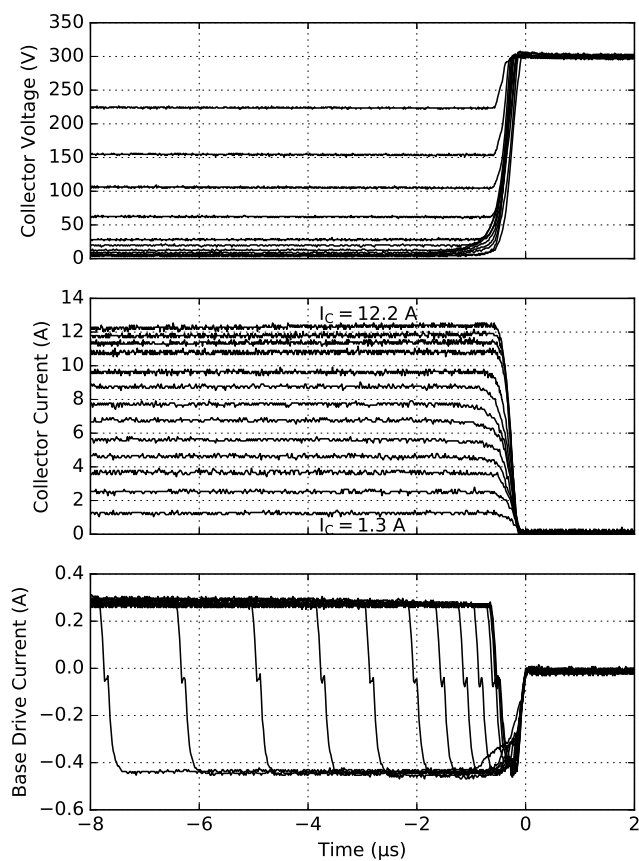


Fig. 8. i_{++i}

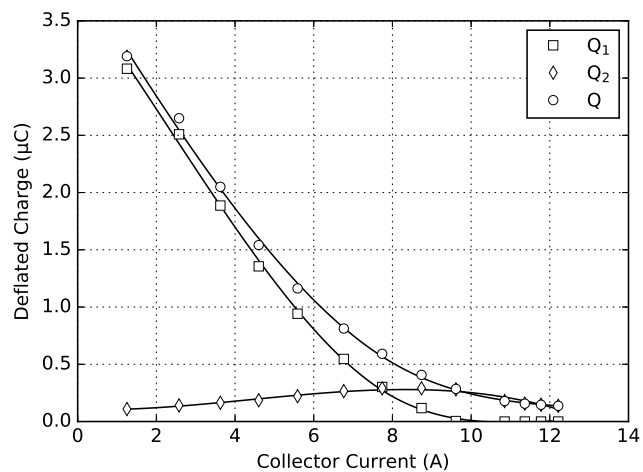


Fig. 9. i_{++i}

- [6] J. Miklas, Power Switching Transistors, Brno: Brno University of Technology, Faculty of Electrical Engineering and Communication. 2016. Head of Diploma Thesis doc. Dr. Ing. Miroslav Patočka
- [7] P. Prochazka, J. Miklas, I. Pazdera, M. Patočka, J. Knobloch, R. Cipin, "Measurement of Power Transistors Dynamic Parameters", Mechatronics 2017, pp.571-577, ISBN 978-3-319-65959-6